

See discussions, stats, and author profiles for this publication at: <https://www.researchgate.net/publication/6931810>

Stereodynamic Effects in the Adsorption of Propylene Molecules on Ag(001)

ARTICLE in THE JOURNAL OF PHYSICAL CHEMISTRY B · JANUARY 2006

Impact Factor: 3.3 · DOI: 10.1021/jp0542571 · Source: PubMed

CITATIONS

11

READS

16

7 AUTHORS, INCLUDING:



Luca Vattuone

Università degli Studi di Genova

117 PUBLICATIONS 2,314 CITATIONS

SEE PROFILE



Mario Rocca

Università degli Studi di Genova

176 PUBLICATIONS 3,231 CITATIONS

SEE PROFILE



David Cappelletti

Università degli Studi di Perugia

151 PUBLICATIONS 3,325 CITATIONS

SEE PROFILE



Franco Vecchiocattivi

Università degli Studi di Perugia

120 PUBLICATIONS 1,782 CITATIONS

SEE PROFILE

Stereodynamic Effects in the Adsorption of Propylene Molecules on Ag(001)

A. Gerbi,[†] L. Vattuone,^{*,†,‡} M. Rocca,^{†,‡} F. Pirani,[§] U. Valbusa,[†] D. Cappelletti,^{||} and F. Vecchiocattivi^{||}*Dipartimento di Fisica, Università Genova and IMEM-CNR Sezione di Genova, Via Dodecaneso 33, Genova, Italy, and Dipartimento di Chimica and Dipartimento di Ingegneria Civile ed Ambientale, Università di Perugia, Via Elce di Sotto, Perugia, Italy**Received: August 1, 2005; In Final Form: October 7, 2005*

We report on the experimental evidence of the role of rotational alignment of the gas-phase molecules in the interaction of propylene with Ag(001). Molecular alignment has been controlled by a velocity selection of the impinging molecules, flying in a supersonic seeded molecular beam. The experimental findings indicate that at low surface coverage the sticking probability is independent of molecular alignment, while when coverage exceeds few percent of a monolayer, molecules impinging rotating parallel to the surface (helicopter-like configuration) achieve a higher chance to be trapped than those which impinge rotating perpendicularly (cartwheels). The sudden appearance of a large stereodynamic effect suggests that the adsorption proceeds via a mobile precursor state and is tentatively correlated with a change in the configuration of the added propylene molecules, which adsorb tilted rather than flat at the surface.

I. Introduction

The role of molecular orientation has often been postulated to be relevant in the adsorption dynamics of gas molecules at surfaces.¹ However, most experimental investigations focused to date on the determination of the quantum state of molecules desorbing or scattered off the surface and recovered information on the quantum-state dependence of the sticking probability, S , by detailed balance arguments.² Only a few experiments³ measured directly the dependence of the adsorption probability on the molecular orientation: they employed exclusively molecular beams of symmetric top polar molecules oriented by electrostatic techniques and resolved the difference in the interaction of the two different molecular ends with the surface.^{4,5}

Recently, the collisional alignment of the rotational angular momentum \mathbf{J} , occurring in the supersonic expansion of a seeded beam and associated with the propensity of molecules to populate specific rotational states,^{6–8} has been successfully employed by us to investigate stereodynamical effects in adsorption of ethylene, a nonpolar molecule, on an oxygen precovered Ag(001) surface.^{9,10} In particular, we found the initial value of the sticking S_0 to be independent from the alignment of the impinging molecules. Moreover, we discovered a threshold in the ethylene coverage above which the uptake curves for molecules rotating, respectively, nearly parallel (helicopters) and nearly perpendicular (cartwheels) to the surface depart, with the cartwheels having a higher chance to be scattered back into the gas phase.

We show here that a similar effect is also observed for the interaction of propylene with Ag(001), thus supporting the picture that the anisotropy in S , observed at intermediate hydrocarbon coverage, results from stereodynamic effects which

selectively drive collisions between already adsorbed molecules (exhibiting a well-defined orientation) and molecules trapped in a mobile precursor and maintaining memory of their initial alignment while moving along the surface (rotationally non-thermalized precursor). Therefore, we demonstrate here that the existence of a steric anisotropy in the adsorption process is not a peculiarity of the ethylene–Ag system but most probably a general feature of weakly interacting systems.

II. Experimental Section

A. Experimental Setup. The experiments have been performed in an ultrahigh vacuum (UHV) chamber (main chamber) operated at a base pressure of 2×10^{-10} mbar, where a seeded supersonic molecular beam impinges (in these investigations, perpendicularly) on an Ag(001) surface cooled to 110 K. For a detailed description of the apparatus, see ref 11. In the following, only some aspects concerning the production of the supersonic molecular beam and a recent improvement on its velocity analysis will be discussed. The production of supersonic beams involves three differentially pumped stages, separated by skimmers and collimators. High-purity propylene seeded in high-purity helium (96% He), at a total stagnation pressure of about 2 bar, expands through a ceramic nozzle of 80 μm diameter, which can be heated to 900 K even when employing reactive gases. The gas temperature at the nozzle T_N has been determined as described in ref 12. A compact two-disk mechanical velocity selector, inserted in the second pumping stage¹³ and rotating at controlled frequency, has been employed to separate the slow (ST) from the fast (FT) tails of the velocity distribution of the emerging supersonic seeded beam: it has been, in fact, demonstrated^{6–8} that molecules such as O_2 , N_2 , benzene, ethylene, and acetylene flying in ST and FT exhibit a different degree of alignment. Since a direct, quantitative information for C_3H_6 molecules in supersonic expansions is lacking, the present experiments have been planned by assuming that C_3H_6 achieves, under the same beam source conditions, a velocity-dependent collisional alignment very similar to the one measured

* Corresponding author. E-mail: vattuone@fisica.unige.it.

[†] Dipartimento di Fisica, Università Genova.

[‡] IMEM-CNR Sezione di Genova.

[§] Dipartimento di Chimica, Università di Perugia.

^{||} Dipartimento di Ingegneria Civile ed Ambientale, Università di Perugia.

for lighter hydrocarbons (C_2H_2 and C_2H_4).⁸ This parameter is therefore controlled indirectly by velocity-analyzing the generated seeded beams.

To maintain the beam flux in the main chamber high enough to perform direct uptake experiments, the design of the velocity selector is optimized to allow a high transmission of the molecular beam. As a consequence, the experimental device shows a limited velocity resolution,¹³ whose characterization involves a detailed knowledge of the employed experimental conditions and requires a proper calibration.

A collimator, placed between the third stage and the main chamber, limits the angular divergence of the molecular beam to 0.16° (hwhm, half-width at half-maximum), thus ensuring the spatial distribution of the molecules at the crystal to be uniform over the spot illuminated by the beam and to be independent of the rotational frequency of the mechanical velocity selector. The high angular resolution also ensures a spot at the sample position smaller than the sample size, as checked by dosing molecular oxygen on Pd(100): in this case, adsorption leads, at high oxygen coverage, to the formation of ordered structures evident from inspection by low energy electron diffraction (LEED). LEED inspection can thus be used to determine the shape of the spot illuminated by the molecular beam at the sample position. The beam has a trapezoidal profile with longer and shorter bases close in length, as indicated by the small relative area (less than 9%) of the surface with a lower oxygen coverage (and a different LEED structure), which separates the center of the spot from the part of the sample not illuminated by the molecular beam. A quadrupole mass spectrometer (QMS) in the main chamber, not in line of sight with the beam, has been used as a residual gas analyzer and to measure the beam intensity. The latter has been employed for the calibration of the selector as velocity analyzer and alignment controller and for determining the sticking probability.

B. Beam Velocity Analysis. The full beam intensity of a pure propylene beam (100% C_3H_6) has been measured by a spinning rotor gauge, with the selector removed off the beam path. The intensity of the velocity-selected seeded beam has then been obtained by comparing the partial pressure rise in the main chamber to that of a nonselected pure propylene beam (0.099 ML/sec; 1 ML = 1.1810^{15} molecules/cm², which is the atomic density at the Ag(100) surface). More details on the adopted procedure are given in ref 14, where a recent investigation of propylene adsorption dynamics, carried out by coupling molecular beam (without velocity selection) and vibrational spectroscopy techniques, is described.

Herein, the velocity selector has been calibrated by measuring the partial C_3H_6 pressure variations in the UHV chamber as a function of its rotational frequency, f . The results for a supersonic molecular beam of C_3H_6 seeded in He, emerging from a source operated at room temperature (300 K), are shown in the lower panel of Figure 1. The molecular beam intensity exhibits an oscillatory behavior corresponding to the opening, through the selector, of successive helical paths of different orders n . As shown in detail in ref 13, the possibility of selecting the velocity distribution with a specific n involves the choice of f in a particular range and determines specific resolution conditions. The maxima in the transmitted beam intensity always correspond to the selection of the (more intense) central part of the velocity distribution, close to the peak velocity (PV), while ST and FT can be alternatively sampled by varying f of $\sim \pm 10\%$ (see Figure 1), as done previously in similar experiments with C_2H_4 .^{9,10} In the present experiments, the typical flux for selected

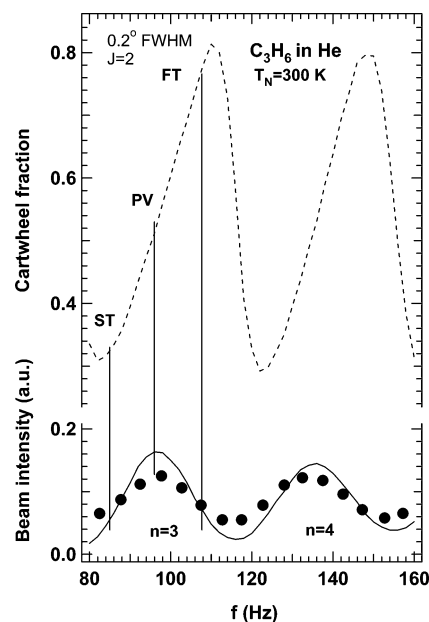


Figure 1. Molecular beam intensity (circles) recorded as a function of the rotational frequency f of the velocity selector. Oscillations in the signal correspond to the opening of the helical paths of orders $n = 3$ and $n = 4$ (see text). The results of a Monte Carlo simulation performed for a fwhm of 0.2° are also shown: the continuous line is the intensity transmitted through the velocity selector, while the dashed line represents the relative weight of molecules flying as cartwheels, obtained by assuming C_3H_6 as a linear molecule in the $J = 2$ rotational level and averaging over the selector transmission function and over the beam divergence.

ST and FT is on the order of ~ 0.005 ML/s, while it is about twice as large for PV.

To investigate the role of the kinetic energy E of the impinging molecules, seeded molecular beams have been generated by heating the nozzle, and their intensity has been measured as a function of f for different T_N . Data for $T_N = 358$ and 475 K are reported in Figure 2 and compared with those measured at room temperature. The most probable translational energy E_{PV} , typical of molecules belonging to PV, was evaluated through the usual relation

$$E_{PV} = \frac{m}{\langle m \rangle} \left(\frac{\gamma}{\gamma - 1} \right) k T_N \quad (1)$$

where m is the propylene molecular mass, $\langle m \rangle$ the average mass of the gas mixture, γ the ratio of constant pressure to constant volume specific heats, and k the Boltzmann constant. The changes in E_{PV} due to the increase of T_N are consistent with the relative frequency shifts in the intensity maxima equal to $\sim 7\%$ for $T_N = 358$ K and to $\sim 30\%$ for $T_N = 475$ K, as measured during the beam velocity analysis with $n = 3$ (see Figure 2).

The most probable energies E_{ST} and E_{FT} of the selected ST and FT cannot be directly deduced from the corresponding rotational frequency f of the mechanical velocity selector, because of its limited resolution conditions, and was therefore estimated by a Monte Carlo simulation. First, the experimental dependence of the molecular beam intensity on f was fitted to reproduce the position of the maxima, thus determining the calibration of the frequency/velocity scale. This calibration has then been inserted, together with the geometrical features of the mechanical velocity selector and with the angular divergence of the beam, in successive simulations aimed at characterizing the transmitted distributions. Such an analysis, providing at any

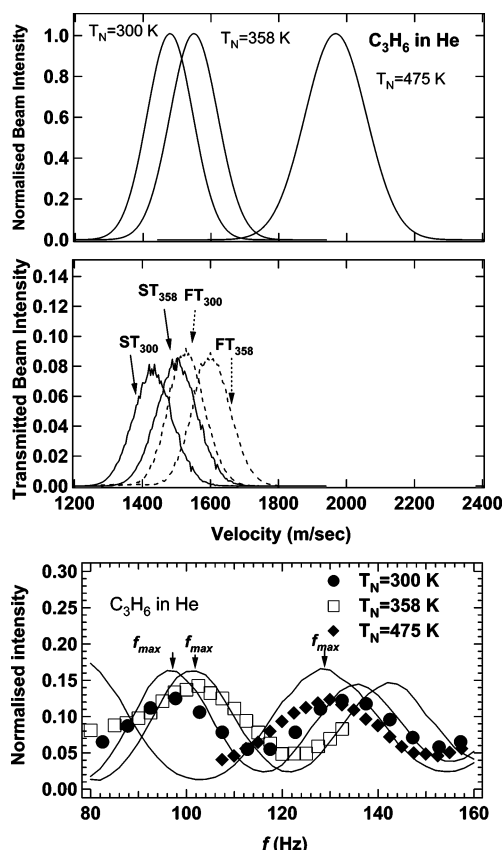


Figure 2. Lower panel: the beam intensity measured as a function of the rotational frequency f of the mechanical velocity selector and for different nozzle temperature T_N . The lines represent Monte Carlo simulations. Central panel: portions of the velocity distributions, effectively transmitted by the selector, at the indicated conditions, as suggested by the Monte Carlo analysis. Upper panel: velocity distribution of three seeded beams, emerging from gas expansion at the indicated nozzle temperatures.

f the portion of the velocity distribution effectively transmitted by the selector, was focused mainly on the f values chosen to select ST and FT. Some results of the simulations are reported in the central panel of Figure 2. The same procedure was used to predict the relative weight of the cartwheel-like molecules in the beam selected at each f , assuming that C_3H_6 aligns in the same way as C_2H_4 and C_2H_2 .^{8,10} The obtained results are plotted in the upper part of Figure 1.

It is of relevance to note that the extension to the present C_3H_6 system of the terminology *helicopter* and *cartwheel*, introduced to describe the approach of a rotating diatomic or linear molecule to a surface, is not straightforward. Propylene is an asymmetric top molecule, which behaves only approximately as a linear top, with two of the moments of inertia being much larger than the third. However, for the sake of simplicity and as done for the ethylene case,^{9,10} we define as *cartwheels* those molecules rotating perpendicularly or nearly perpendicularly with respect to the surface plane and as *helicopters* those rotating parallel or nearly parallel to it. Detailed information on the rotational state distribution for propylene is not available. The seeding effect ensures that the molecules in the beam mostly populate the lowest J states because of the rotational cooling occurring in the supersonic expansion. The width of the velocity distribution provides an estimate of the rotational temperature, and from the analogy with the better characterized cases of acetylene and ethylene seeded in He,⁸ it can be assumed that with a room-temperature nozzle the states with $1 \leq J \leq 3$ are the most populated.

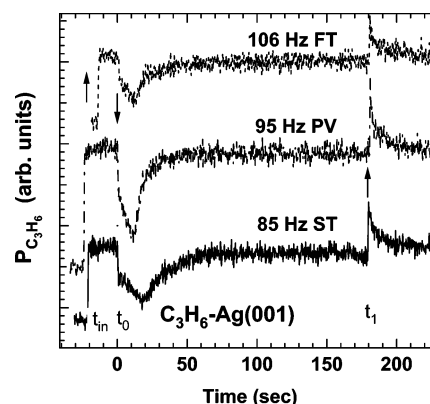


Figure 3. Propylene partial pressure for several KW experiments performed by selecting the slow (ST, continuous), fast (FT, dotted) and the central (PV, dash-dotted) portions of the velocity distribution. The traces are vertically shifted to avoid superpositions.

The rotational alignment is confirmed a posteriori by the analysis of the sticking coefficient measurements, performed under various conditions (see next section) with velocity-selected beams.

C. Absorption Measurements with Velocity-Selected Beams.

The sticking probability has been measured by the well-known King and Wells method¹⁵ (KW). In Figure 3, typical pressure traces are shown, recorded with the residual gas analyzer (QMS) tuned at $m/e = 41$, one of the main peaks in the propylene mass spectrum. The abrupt increase of the propylene partial pressure, $P_{C_3H_6}$, at time t_{in} corresponds to the admittance of the molecular beam into the main chamber, while an inert flag prevents it from striking the sample. At time t_0 , the flag is removed and the beam hits the bare surface: the decrease in $P_{C_3H_6}$ is due to its gettering action. The ratio between the pressure drop observed starting from t_0 (molecular beam striking the sample) and the pressure increase observed at time t_{in} (beam intercepted, sample not exposed) is a direct measure of the sticking probability as a function of time. At a later time t_1 , the flag is inserted again in the beam path and a transient desorption is observed, indicating that some of the ad-molecules are not stable at the sample temperature, $T = 110$ K.^{14,16} A similar experiment performed under the same conditions, but inserting the flag at an earlier time after the beginning of the exposure, showed no desorption, indicating that the molecules end up initially into a more strongly bound state.

The three different pressure traces reported in Figure 3 have been measured by sampling molecules flying in ST (continuous), in PV (dash dotted), and in FT (dotted) of the velocity distribution of the seeded C_3H_6 molecular beam generated at $T_N = 300$ K. It is important to restate that, as shown in Figure 1, both the relative weight of cartwheels and kinetic energy E are expected to regularly increase when passing from ST to PV and FT. Measurements carried out under selected experimental conditions have been used to separate the different dependencies (see next section).

III. Results and Discussion

The integration of the missing pressure in the uptake curves of Figure 3 provides the dependence of the sticking probability S on the surface coverage Θ . An example of the results, reported in Figure 4, shows that S_0 , corresponding to $\Theta = 0$, is the same for ST, PV, and FT. Furthermore, S increases with Θ until a certain coverage $\Theta(S_{max})$ is reached and decreases eventually: the value of $\Theta(S_{max})$ depends critically on the selected part of the velocity distribution.

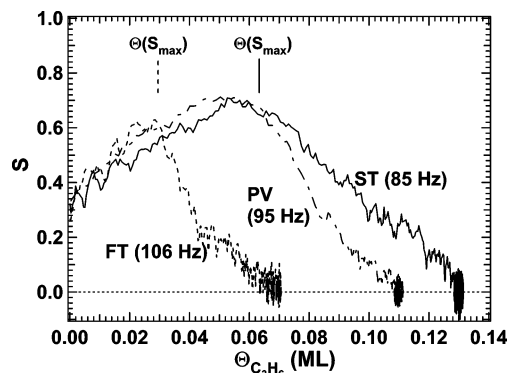


Figure 4. Sticking probability S vs surface coverage Θ for different rotational frequencies of the velocity selector, obtained from the analysis of the curves of the previous figure. The vertical lines indicate $\Theta(S_{\max})$.

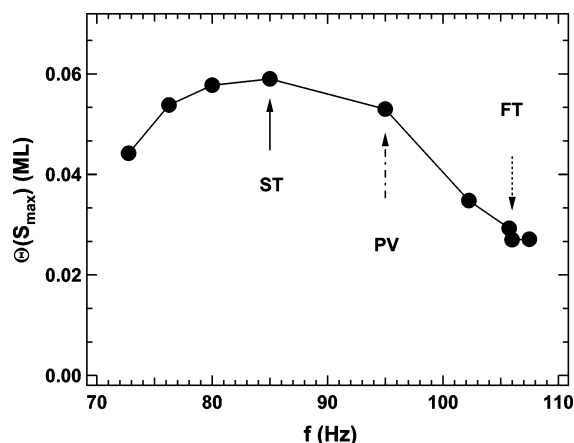


Figure 5. Surface coverage for which the sticking is maximum, $\Theta(S_{\max})$, vs frequency f of the velocity selector. Data refer to a supersonic molecular beam of propylene seeded in He exploiting a room-temperature nozzle.

Further experiments were carried out at different rotational frequencies f of the selector and are summarized in Figure 5. Clearly, $\Theta(S_{\max})$ is largest when selecting molecules in ST, while it decreases smoothly with f . It is of interest to note that, when selecting PV, $\Theta(S_{\max})$ is only slightly smaller than for ST, even if the beam intensity is twice as large. This implies that, under the present conditions, the beam flux does not significantly affect the observed anisotropy in the sticking probability. For PV, the alignment degree is intermediate between the ST and FT cases (although closer to that in ST), in qualitative agreement with what was anticipated in Figure 1.

Measurements of S_0 and $\Theta(S_{\max})$, obtained from uptake experiments performed at different E , are shown in Figure 6, where they are compared with those achieved by using beams of pure C_3H_6 . It is apparent that possible small differences in S_0 between ST and FT are at the limit of the present experimental sensitivity, with S_0 being perhaps only slightly larger for FT. A significant difference, well above the experimental error, is present, on the contrary, for $\Theta(S_{\max})$.

To make such delicate points more evident, we compare in Figure 7 the coverage dependence of S measured for two beams having nearly the same E (~ 0.52 eV), obtained by sampling FT ($T_N = 300$ K, dotted) and ST ($T_N = 358$ K, continuous). It is evident that ST leads to a much higher total uptake than FT. By using arguments similar to those in ref 12, where the rotational temperature T_{rot} was estimated to be around 12 K for a seeded beam of ethylene at $T_N = 300$ K, and taking into account the variation of 58 K in T_N , we can evaluate whether

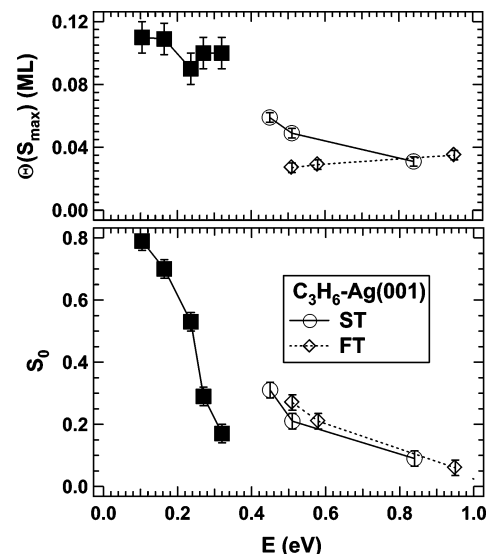


Figure 6. $\Theta(S_{\max})$ (upper panel) and S_0 (lower panel) as a function of collision energy E . Data are shown for a molecular beam of pure propylene, not velocity selected (squares), and for the ST (open circles) and FT (open diamonds) of a supersonic molecular beam seeded in He at various nozzle temperatures.

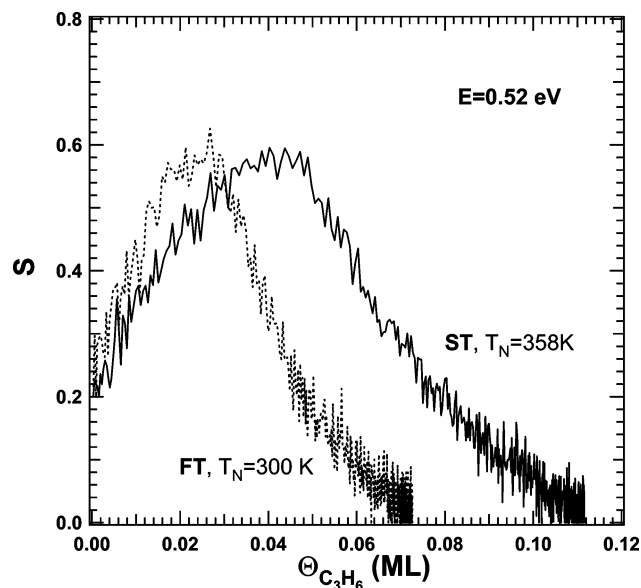


Figure 7. Sticking probability vs surface coverage at a collisional energy of 0.52 eV. Dotted curve: FT of a molecular beam produced at $T_N = 300$ K. Continuous curve: ST of a molecular beam generated at $T_N = 358$ K.

the corresponding change in T_{rot} does not exceed 3 K. Therefore, the effect shown in Figure 7 should mostly arise from a variation in the molecular alignment and be only slightly influenced by the change in T_{rot} . Moreover, such an influence would go in the direction opposite to experimental evidence, since as demonstrated both for ethylene¹² and propylene,¹⁴ rotationally hot molecules have a lower trapping probability than cold molecules with the same translational energy.

All these experimental findings are not inconsistent with our starting hypothesis, i.e., that C_3H_6 molecules in seeded supersonic expansions show a degree and a velocity dependence of the collisional alignment close to those observed for lighter hydrocarbons.⁸ Moreover, we note that the present data for the sticking anisotropy of propylene are similar to those of ethylene on O_2 precovered Ag(001).^{9,10}

First, the substantial independence of S_0 on the selected beam velocity indicates that the observed anisotropy in the sticking does not arise from the interaction between incoming propylene and the bare Ag(001) surface. Possible small differences in S_0 may suggest that cartwheeling molecules, which undergo effective translational to rotational energy transfer, adsorb slightly better than helicopters when colliding with the bare surface (in accord, e.g., with refs 17 and 18). This effect is small, however, when compared to the large difference observed at intermediate coverage.

Second, S increases by more than a factor of three when the coverage changes from zero to less than 0.04 ML. This can be explained by either assuming that the ad-molecules modify the properties of the neighboring sites located in an area of about three atomic spaces around them or, more reasonably, that an impinging molecule enters into a *nonthermal precursor state*, which maintains the memory of some features of the gas-phase state, such as kinetic energy and rotational alignment. The behavior of a molecule in the precursor state becomes crucial when hitting a preadsorbed propylene molecule to which it transfers its excess energy, becoming definitely stuck. From the slope of the $S(\Theta)$ curve, we infer that on the average about seven sites may be visited by a molecule during its permanence in such precursor state. Notably, the increase in $S(\Theta)$ is missing for pure beam experiments:¹⁴ in this case, the kinetic energy is smaller by more than a factor of four (see Figure 6), the molecular alignment is strongly reduced, and the rotational relaxation is less effective.

The increase of S with coverage becomes even larger if the energy is further increased (see ref 14), thus confirming our hypothesis that adsorbate-assisted adsorption is due to collisions between molecules in the precursor state and already chemisorbed ethylene. The change in corrugation of the gas surface potential with increasing coverage, recently invoked to account for adsorbate-assisted adsorption,¹⁹ cannot account for the large initial slope of the $S(\Theta)$ curve observed here. Such a slope can, on the other hand, be rationalized by assuming that temporarily trapped molecules can more easily get rid of their residual energy and get definitely stuck when colliding with a chemisorbed molecule having the same mass.¹⁴

The observed difference between helicopters and cartwheels can only arise from an anisotropy in the collision dynamics between already adsorbed propylene and propylene molecules in the precursor state. Reasonably, cartwheels get trapped after converting some of their translational energy into rotational energy so that they still continue to rotate nearly perpendicularly to the surface. In this configuration, they can also undergo further rotationally inelastic collisions. Helicopters, on the other hand, tend to rotate and move parallel to the surface. Thus, they have a lower chance to be scattered back into the gas phase when the trapped molecules collide against another, preadsorbed, propylene.

It remains to be explained why the anisotropy in S starts abruptly at such a small coverage.

This fact cannot in our opinion be explained by invoking the role of defects for two reasons. First, the coverage at which the anisotropy shows up, though low, would correspond to an exceedingly large defect density (the 0.1° miscut angle could account only for some thousandths of a monolayer and not for some percent). Second, since defect sites are almost always populated first, the sticking probability should decrease with respect to its initial value, until the coverage corresponding to the concentration of defects is reached, contrary to experimental evidence.

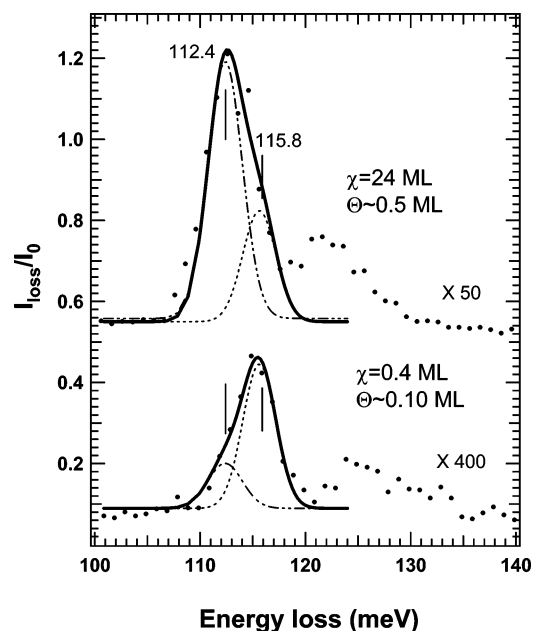


Figure 8. HREEL spectra, from ref 14, showing the shift in the wag mode of propylene adsorbed on bare Ag(001) from 115 to 112 meV with increasing exposure χ . The fit with two Gaussians plus a constant enlightens the contribution of the low- and high-frequency components of the wag mode to the total intensity. The 112 meV moiety (assigned to a tilted species) is present already after an exposure of only 0.4 ML at 0.48 eV (performed with an unselected beam), for which the total coverage Θ reads about 0.10 ML.

Vibrational spectroscopy measurements for propylene on Ag-(110)^{20,21} and on Ag(001)¹⁴ demonstrate that this molecule adsorbs in two different states, identified on Ag(110) by two different IR peaks at 113 and 115 meV for the wag motion. At low coverage, the high-frequency species, assigned to a flat-lying moiety, dominates. With increasing coverage, the low-frequency peak, assigned to a tilted configuration, initially equates and, above 0.10 ML, overcomes the other component of the doublet. On Ag(100), a shift of the loss peak of the wag vibration from 115 to 112 meV with increasing exposure χ takes place as shown by the HREEL (high-resolution electron energy loss spectroscopy) spectrum reported in Figure 8. Fitting of the loss feature in the 110–120 meV region, with two Gaussian functions plus a constant (accounting for the background), demonstrates that it consists therefore of two unresolved components, with a behavior similar to that of the doublet observed on Ag(110).¹⁴ The change in the HREEL spectra for propylene on Ag(100) correlates with the onset of the stereodynamic effect in the uptake curves reported above. We suggest therefore that the flat-lying chemisorbed moiety, dominating at low coverage, is insensitive to the rotational alignment of the nonthermal molecules which move along the surface. On the contrary, the tilted species, which dominates only at larger coverage but is clearly present already at 0.10 ML (see shoulder in lower spectrum of Figure 8, which can be assigned to a small-intensity component at ~112 meV), may cause trapped cartwheels to scatter off into the gas phase more easily than helicopters, thus justifying the onset of steric anisotropy.

IV. Conclusions

We have investigated the adsorption of propylene on an Ag-(001) surface by scattering of a velocity-selected molecular beam, at normal incidence on the target. The velocity selection also provides an indirect control a posteriori of the molecular

alignment in the beam and thus the possibility of revealing stereodynamical effects.

The experimental findings suggest that the adsorption process is mediated by a nonthermal precursor state which survives long enough to allow molecules to sample, on the average, at least seven sites around the initial impact position. Molecules in such a state are not thermalized and maintain the memory of their orientation with respect to the surface: their collision dynamics with the clean surface and with adsorbed molecules at low coverage (flat-lying chemisorbed) appears to be substantially independent of the rotational alignment. Another adsorption state exists and corresponds most probably to a tilted configuration of the ad-molecules. When, at about 0.05 ML, the population in such a tilted state starts to be important, a large stereodynamic effect is observed favoring adsorption of helicopters with respect to cartwheels. We explain this result by picturing that cartwheels may be more easily backscattered into the gas phase via rotational to translational energy conversion when colliding with tilted, already chemisorbed, propylene molecules.

References and Notes

- (1) Hou, H.; Guilding, S. J.; Rettner, C. T.; Wodtke, A. M.; Auerbach, D. J. *Science* **1990**, 277, 80.
- (2) Weida, M. J.; Sperhac, J. M.; Nesbitt, D. J. *J. Chem. Phys.* **1996**, 105, 749.
- (3) Sitz, G. O. *Rep. Prog. Phys.* **2002**, 65, 1165.
- (4) Kuipers, E. W.; Tenner, M. G.; Kleyn, A. W.; Stolte, S. *Nature (London)* **1988**, 334, 420.
- (5) Curtis, T. J.; Bernstein, R. B. *Chem. Phys. Lett.* **1989**, 161, 212.
- (6) Curtiss, T. J.; MacKay, R. S.; Bernstein, R. B. *J. Chem. Phys.* **1990**, 93, 7387.
- (7) Ionov, S. I.; La Villa, M. E.; Bernstein, R. B. *J. Chem. Phys.* **1990**, 93, 7416.
- (8) Brandt, M.; Muller, H.; Zagatta, G.; Wehmeyer, O.; Bowering, N.; Heinzmann, U. *Surf. Sci.* **1995**, 331–333, 30.
- (9) Aquilanti, V.; Ascenzi, D.; Cappelletti, D.; Pirani, F. *Nature (London)* **1994**, 371, 399.
- (10) Aquilanti, V.; Ascenzi, D.; Cappelletti, D.; Fedeli, R.; Pirani, F. *J. Phys. Chem.* **1997**, A101, 7648.
- (11) Pirani, F.; Cappelletti, D.; Bartolomei, M.; Aquilanti, V.; Scotoni, M.; Vescovi, M.; Ascenzi, D.; Bassi, D. *Phys. Rev. Lett.* **2001**, 86, 5035.
- (12) Bartolomei, M. Ph.D. Thesis. Università di Perugia, 2002; <http://leo.tech.ing.unipg.it/TESI/tesimax.pdf>.
- (13) Aquilanti, V.; Bartolomei, M.; Pirani, F.; Cappelletti, D.; Vecchiocattivi, F.; Shimizu, Y.; Kasai, T. *Phys. Chem. Chem. Phys.* **2005**, 7, 291.
- (14) Vattuone, L.; Gerbi, A.; Rocca, M.; Valbusa, U.; Pirani, F.; Cappelletti, D.; Vecchiocattivi, F. *Angew. Chem. Int. Ed.* **2004**, 43, 5200.
- (15) Vattuone, L.; Gerbi, A.; Rocca, M.; Valbusa, U.; Pirani, F.; Cappelletti, D.; Vecchiocattivi, F. *J. Chem. Phys.*, in press.
- (16) Rocca, M.; Valbusa, U.; Gussoni, A.; Maloberti, G.; Racca, L. *Rev. Sci. Instrum.* **1991**, 62, 2171.
- (17) Vattuone, L.; Valbusa, U.; Rocca, M. *Phys. Rev. Lett.* **1999**, 82, 4878.
- (18) Pirani, F.; Cappelletti, D.; Vecchiocattivi, F.; Vattuone, L.; Gerbi, A.; Rocca, M.; Valbusa, U. *Rev. Sci. Instrum.* **2004**, 75, 349.
- (19) Gerbi, A.; Savio, L.; Vattuone, L.; Rocca, M. *J. Chem. Phys.* **2005**, 122, 134701.
- (20) King, D. A.; Wells, M. G. *Surf. Sci.* **1972**, 29, 454.
- (21) Arumainayagam, C. R.; McMaster, M. C.; Madix, R. J. *J. Vac. Sci. Technol., A* **1991**, 9, 1581.
- (22) Stinnett, J. A.; Weaver, J. F.; Madix, R. J. *Surf. Sci.* **1998**, 395, 148.
- (23) Stinnett, J. A.; Madix, R. J.; Tully, J. C. *J. Chem. Phys.* **1996**, 104, 3134.
- (24) Carlsson, A. F.; Madix, R. J. *J. Chem. Phys.* **2000**, 113, 838.
- (25) Pamela-Crew, J.; Madix, R. J. *J. Chem. Phys.* **1996**, 104, 1699.
- (26) Solomon, J. L.; Madix, R. J.; Stöhr, J. *J. Chem. Phys.* **1990**, 93, 8379.